

Mixed conductivity, thermal expansion and defect chemistry of A-site deficient $\text{LaNi}_{0.5}\text{Ti}_{0.5}\text{O}_{3-\delta}$

S. Yakovlev*, V. Kharton, A. Yaremchenko, A. Kovalevsky, E. Naumovich, J. Frade

Department of Ceramics and Glass Engineering, University of Aveiro, 3810-193 Aveiro, Portugal

Available online 19 March 2007

Abstract

This work is focused on the analysis of defect chemistry and partial electronic and oxygen ionic conductivities of A-site deficient $\text{La}_{1-x}\text{Ni}_{0.5}\text{Ti}_{0.5}\text{O}_{3-\delta}$ ($x=0.05$ and 0.10). The orthorhombic-to-rhombohedral phase transition was monitored by means of dilatometry and high-temperature X-ray diffraction. The average thermal expansion coefficients vary in the range $(8.5\text{--}13.0) \times 10^{-6} \text{ K}^{-1}$, increasing with temperature and A-site deficiency. The ion transference numbers determined by the Faradaic efficiency measurements are lower than 0.1% at $900\text{--}975^\circ\text{C}$ in air. Activation energies of the oxygen ionic conductivity at $897\text{--}977^\circ\text{C}$ are 430 and 220 kJ/mol for $x=0.05$ and 0.10 , respectively. Atomistic simulation demonstrated high stability of ternary defect clusters formed by the vacant sites in the A-sublattice, oxygen vacancies and Ni^{3+} cations, which leads to a very low level of mixed conductivity.

© 2007 Elsevier Ltd. All rights reserved.

Keywords: Defects; Thermal expansion; Ionic conductivity; Perovskites; Membranes; Transition metal oxides

1. Introduction

Nickel-containing mixed oxygen-ionic and electronic conductors with perovskite-like structure are of interest as materials of oxygen-permeable ceramic membranes and as catalyst precursors for natural gas conversion processes.^{1,2} Perovskite-type $\text{LaNiO}_{3-\delta}$ possesses a low thermodynamic stability and decomposes on heating or reducing oxygen partial pressure with formation of nickel oxide and Ruddlesden-Popper $\text{La}_{1+n}\text{Ni}_n\text{O}_{3n+1}$ phases. Co-existence of Ni and perovskite-type structure results in high catalytic activity of the system due to interaction with metal and oxidation of carbon by oxygen migrating from the lattice.² To some extent, stability of perovskite structure can be improved by the extensive substitution of nickel with other transition metal cations having lower reducibility (Cr, Mn, Ti, etc.).³

The present work was focused on the evaluation of the effect of A-site nonstoichiometry on thermal expansion, defect chemistry and transport properties of $\text{La}_{1-x}\text{Ni}_{0.5}\text{Ti}_{0.5}\text{O}_{3-\delta}$ ($x=0.05$ and 0.1). In the parent compound, $\text{LaNi}_{0.5}\text{Ti}_{0.5}\text{O}_{3-\delta}$, all Ni cations are divalent and the electronic transport occurs presumably via hopping of p-type charge carriers.⁴ Introducing A-site

deficiency is expected to result in higher concentration of the oxygen vacancies and/or holes. The information on the behavior of such defects in the A-site nonstoichiometric compounds is, however, scarce and contradictory. The oxygen ionic transport may increase with A-site deficiency due to the increase of the oxygen vacancy concentration (according to the neutrality conditions) and due to random distribution of the vacant sites in the cation sub-lattice suppressing ordering in the oxygen sub-lattice.^{5,6} On another hand, local structural distortions and association of the oxygen and cation vacancies can result in deterioration of transport properties of ceramics.⁷ In the present work, atomistic computer simulations were carried out in order to clarify the defect interaction mechanisms.

2. Experimental

Powders of $\text{La}_{1-x}\text{Ni}_{0.5}\text{Ti}_{0.5}\text{O}_{3-\delta}$ ($x=0.05$ and 0.10) were synthesized employing conventional solid state reaction technique. High-purity $\text{La}(\text{NO}_3)_3 \cdot 6\text{H}_2\text{O}$, $\text{Ni}(\text{NO}_3)_2 \cdot 6\text{H}_2\text{O}$ and TiO_2 were used as raw materials. The solid-state reactions were conducted in air at $1000\text{--}1100^\circ\text{C}$ for 6 h with multiple intervening grinding steps. Dense samples were uniaxially pressed and sintered at $1520\text{--}1540^\circ\text{C}$ in air for 15 h with slow cooling. Microstructure and phase composition of ceramic samples were investigated using scanning electron microscopy (SEM) and X-ray diffraction (XRD) analysis. Structural parameters were

* Corresponding author. Tel.: +351 234 370263; fax: +351 234 425300.
E-mail address: iakovlev@cv.ua.pt (S. Yakovlev).

Table 1
Properties of $\text{La}_{1-x}\text{Ni}_{0.5}\text{Ti}_{0.5}\text{O}_{3-\delta}$ ceramics

Composition	Density (g cm^{-3})	Unit cell parameters	Average TEC	
			T ($^{\circ}\text{C}$)	$\bar{\alpha}$ ($\times 10^{-6} \text{ K}^{-1}$)
$\text{La}_{0.95}\text{Ni}_{0.5}\text{Ti}_{0.5}\text{O}_{3-\delta}$	5.94	$a = 5.5491 \pm 0.0004 \text{ \AA}$	17–527	8.55 ± 0.02
		$b = 5.5503 \pm 0.0004 \text{ \AA}$	527–927	9.99 ± 0.01
		$c = 7.8386 \pm 0.0005 \text{ \AA}$	1027–1227	11.96 ± 0.01
		$V = 241.423 \pm 0.031 \text{ \AA}^3$		
$\text{La}_{0.90}\text{Ni}_{0.5}\text{Ti}_{0.5}\text{O}_{3-\delta}$	6.18	$a = 5.5487 \pm 0.0002 \text{ \AA}$	27–527	9.30 ± 0.02
		$b = 5.5473 \pm 0.0002 \text{ \AA}$	527–827	10.00 ± 0.01
		$c = 7.8374 \pm 0.0002 \text{ \AA}$	927–1097	13.00 ± 0.01
		$V = 241.207 \pm 0.007 \text{ \AA}^3$		
	Total conductivity		Oxygen-ionic conductivity	
	T ($^{\circ}\text{C}$)	E_a (kJ mol^{-1})	T ($^{\circ}\text{C}$)	E_a (kJ mol^{-1})
$\text{La}_{0.95}\text{Ni}_{0.5}\text{Ti}_{0.5}\text{O}_{3-\delta}$	507–1017	89 ± 1	897–977	426 ± 5
$\text{La}_{0.90}\text{Ni}_{0.5}\text{Ti}_{0.5}\text{O}_{3-\delta}$	547–897	90 ± 1	897–977	222 ± 4

refined using the GSAS software.⁸ Thermal expansion was studied by means of dilatometry at a heating rate of $-270 \text{ }^{\circ}\text{C}/\text{min}$. The oxygen nonstoichiometry variations were determined by thermogravimetric analysis (TGA), as described in.⁹ Characterization of transport properties included measurements of the total conductivity (four-probe DC) and oxygen transference numbers (Faradaic efficiency method¹⁰). The GULP software¹¹ was used to perform the atomistic modeling of the structure. Detailed description of the method, successfully used earlier for atomistic computer simulation and analysis of experimental $p(\text{O}_2)$ - T - δ diagrams of perovskite-type $\text{La}_{0.3}\text{Sr}_{0.7}\text{Fe}(\text{M})\text{O}_{3-\delta}$ and $\text{SrFe}(\text{M})\text{O}_{3-\delta}$ ($\text{M} = \text{Al}$ and Ga), can be found elsewhere.¹²

3. Results and discussion

SEM analysis of prepared ceramics revealed no open porosity, cracks or any traces of liquid phase appearance during sintering. Room-temperature XRD analysis of $\text{La}_{0.95}\text{Ni}_{0.5}\text{Ti}_{0.5}\text{O}_{3-\delta}$ ceramics showed formation of single-phase material with orthorhombically distorted perovskite-type structure (space group $Pbnm$), in agreement with data on the parent composition.⁴ The occupancy of the cation sites was calculated by the Rietveld refinement and is found to be very close to nominal; no indication of B-site ordering was revealed. The increase of A-site deficiency up to 10% resulted in the segregation of approx. 2 wt.% of NiO. The lattice parameters are listed in Table 1. Introducing A-site deficiency results in lattice expansion compared to parent compound, $\text{LaNi}_{0.5}\text{Ti}_{0.5}\text{O}_{3-\delta}$ ($a = 5.5171 \text{ \AA}$, $b = 5.5501 \text{ \AA}$, and $c = 7.8562 \text{ \AA}$),⁴ as expected taking into account the higher anion repulsion in A-site deficient structure.

Fig. 1 shows the dilatometric curves of $\text{La}_{1-x}\text{Ni}_{0.5}\text{Ti}_{0.5}\text{O}_{3-\delta}$ ($x = 0.05$ and 0.10); average thermal expansion coefficients (TECs) are given in Table 1. Increasing of the A-site deficiency leads to moderate increase of the TECs values. Thermal expansion is linear, with the exception of anomaly at approximately 977 and 887 $^{\circ}\text{C}$ for $\text{La}_{0.95}\text{Ni}_{0.5}\text{Ti}_{0.5}\text{O}_{3-\delta}$ and

$\text{La}_{0.90}\text{Ni}_{0.5}\text{Ti}_{0.5}\text{O}_{3-\delta}$, respectively (Fig. 1). This effect is associated with the orthorhombic-to-rhombohedral phase transition on heating observed by high-temperature XRD analysis.

The average oxygen nonstoichiometry (δ) and fraction of Ni^{3+} cations ($[\text{Ni}^{3+}]/[\text{Ni}]_{\text{total}}$), calculated from TGA results, were found essentially temperature-independent in the entire temperature range studied (25 – $950 \text{ }^{\circ}\text{C}$), and are equal to 0.04 and 0.13 for $\text{La}_{0.95}\text{Ni}_{0.5}\text{Ti}_{0.5}\text{O}_{3-\delta}$ and 0.11 and 0.14 for $\text{La}_{0.90}\text{Ni}_{0.5}\text{Ti}_{0.5}\text{O}_{3-\delta}$, respectively. Combining the results of TGA and Rietveld refinement, chemical formula for the latter material can be written as $\text{La}_{0.950}\text{Ni}_{0.396}^{2+}\text{Ni}_{0.076}^{3+}\text{Ti}_{0.528}\text{O}_{2.991}$.

The total conductivity of $\text{La}_{0.95}\text{Ni}_{0.5}\text{Ti}_{0.5}\text{O}_{3-\delta}$ in air exhibits a linear Arrhenius behavior in the entire temperature range, as illustrated in Fig. 2. Such dependence is rather atypical for nickel-containing perovskite materials.^{13,14} In the most cases, the total conductivity of Ni-substituted perovskites decreases with increasing temperature due to progressive oxygen losses from the crystal lattice; in particular, $\text{LaNi}_{1-x}\text{Ti}_x\text{O}_{3-\delta}$ ($x < 0.4$) and $\text{LaNi}_{0.5}\text{M}_{0.5}\text{O}_{3-\delta}$ ($\text{M} = \text{Ga}$, Fe , and Co) ceramics exhibit a transition to pseudo-metallic behavior on heating above 327 – $527 \text{ }^{\circ}\text{C}$.^{4,13,14} Obviously, the difference in the conductivity behavior is associated with the temperature-independent oxygen nonstoichiometry of $\text{La}_{1-x}\text{Ni}_{0.5}\text{Ti}_{0.5}\text{O}_{3-\delta}$, as mentioned above.

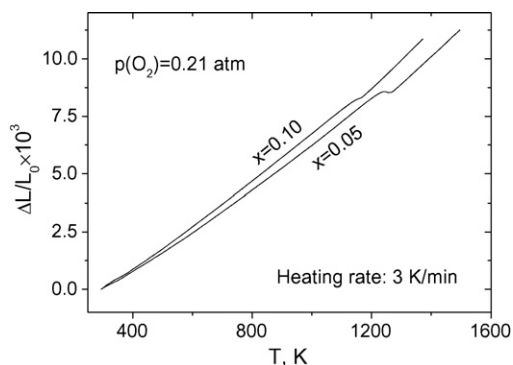


Fig. 1. Dilatometric curves of $\text{La}_{1-x}\text{Ni}_{0.5}\text{Ti}_{0.5}\text{O}_{3-\delta}$ ceramics in air.

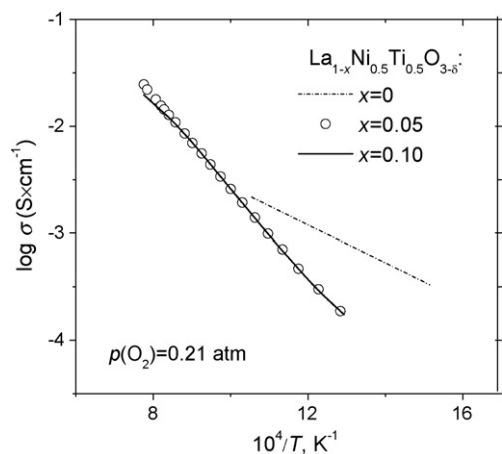


Fig. 2. Total conductivity of $\text{La}_{1-x}\text{Ni}_{0.5}\text{Ti}_{0.5}\text{O}_{3-\delta}$ ceramics in air. The data on $\text{LaNi}_{0.5}\text{Ti}_{0.5}\text{O}_{3-\delta}$ are shown for comparison.

An increase of the A-site deficiency (10% of vacancies in the nominal composition) promotes oxygen losses and results in a slight deviation from the Arrhenius plot at temperatures above 877°C .

The total conductivity of both studied compositions is predominantly electronic; the oxygen ion transference numbers (t_{O}) in air are lower than 0.001. At 727°C , the total conductivity of cation-deficient materials is similar to that of $\text{LaNi}_{0.5}\text{Ti}_{0.5}\text{O}_{3-\delta}$ (Fig. 2), but is characterized with significantly higher activation energy (E_a). Furthermore, the E_a values of $\text{La}_{1-x}\text{Ni}_{0.5}\text{Ti}_{0.5}\text{O}_{3-\delta}$ (Table 1) are higher than expected for a small-polaron mechanism. This may indicate either strong trapping of electronic charge carriers or a broadband conduction mechanism.

The oxygen ionic conductivities (σ_{O}), calculated from the results of Faradaic efficiency and total conductivity measurements, are shown in Fig. 3. For comparison, the data on $\text{Gd}_2\text{Sn}_2\text{O}_7$ ¹⁵ and $(\text{Sm}_{0.9}\text{Sr}_{0.1})_2\text{Ti}_2\text{O}_7$ ¹⁶ pyrochlores are also presented. Two latter materials are characterized with a very low concentration of ionic charge carriers formed due to intrinsic thermal disorder.^{15,16} For $\text{La}_{1-x}\text{Ni}_{0.5}\text{Ti}_{0.5}\text{O}_{3-\delta}$, the oxygen deficiency results from the A-site vacancies charge compensation and is low, but still significant. Nevertheless, the level of ionic transport in $\text{La}_{1-x}\text{Ni}_{0.5}\text{Ti}_{0.5}\text{O}_{3-\delta}$ is lower compared

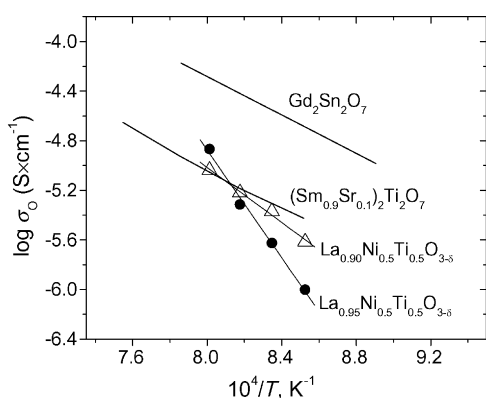


Fig. 3. Temperature dependencies of the oxygen-ionic conductivity of $\text{La}_{1-x}\text{Ni}_{0.5}\text{Ti}_{0.5}\text{O}_{3-\delta}$ ceramics in air. The data on $\text{Gd}_2\text{Sn}_2\text{O}_7$ ¹⁵ and $(\text{Sm}_{0.9}\text{Sr}_{0.1})_2\text{Ti}_2\text{O}_7$ ¹⁶ pyrochlores are shown for comparison.

to $\text{Gd}_2\text{Sn}_2\text{O}_7$ but compatible to $(\text{Sm}_{0.9}\text{Sr}_{0.1})_2\text{Ti}_2\text{O}_7$. One may conclude, therefore, that most oxygen vacancies in the lattice of lanthanum nickelate–titanate are in a trapped state, presumably due to point-defect cluster formation, and do not participate in ionic transport.

In agreement with the results of electronic and ionic transport characterization, the results of the static lattice simulation showed a strong tendency toward localization of the oxygen vacancies near vacant A-site. In most cases, the energetic effects of $V_{\text{A}}''' \cdots V_{\text{O}}''$ pair cluster formation vary in the range from -183 to -76 kJ/mol. The localization of electron holes at the nickel cations surrounding A-site vacancy is also energetically favorable; energy of the cluster formation varies in the narrow range -22 to -35 kJ/mol. For the ternary $V_{\text{A}}''' \cdots V_{\text{O}}'' \cdots \text{Ni}_{\text{B}}^{\text{X}}$ clusters it was observed that their average energy of formation is substantially higher than the sum of corresponding pair-cluster energies and lies in the range -49 to -345 kJ/mol, suggesting a maximum stability of these elements in $\text{La}_{0.95}\text{Ni}_{0.5}\text{Ti}_{0.5}\text{O}_{3-\delta}$. Most likely, formation of such ternary clusters is responsible for the very low ionic and electronic conductivities (Figs. 2 and 3).

4. Conclusions

The charge compensation of A-site deficiency in $\text{La}_{1-x}\text{Ni}_{0.5}\text{Ti}_{0.5}\text{O}_{3-\delta}$ ($x=0.05$ and 0.10) occurs via a mixed mechanism involving formation of Ni^{3+} cations and oxygen vacancies. The oxygen content variations with temperature are very low, indicating a stabilization of trivalent nickel in the lattice of A-site deficient lanthanum nickelate–titanate. $\text{La}_{1-x}\text{Ni}_{0.5}\text{Ti}_{0.5}\text{O}_{3-\delta}$ ceramics exhibit moderate thermal expansion with TECs values in the range $(8.6\text{--}9.3) \times 10^{-6} \text{K}^{-1}$ at $27\text{--}527^\circ\text{C}$ and $(12.0\text{--}13.0) \times 10^{-6} \text{K}^{-1}$ at $927\text{--}1227^\circ\text{C}$. Dilatometric and high-temperature XRD studies revealed an orthorhombic-to-rhombohedral phase transition at 977°C for $\text{La}_{0.95}\text{Ni}_{0.5}\text{Ti}_{0.5}\text{O}_{3-\delta}$ and 887°C for $\text{La}_{0.90}\text{Ni}_{0.5}\text{Ti}_{0.5}\text{O}_{3-\delta}$.

The total conductivity of $\text{La}_{1-x}\text{Ni}_{0.5}\text{Ti}_{0.5}\text{O}_{3-\delta}$ is predominantly electronic with oxygen ionic contribution lower than 0.1% at $900\text{--}975^\circ\text{C}$. The ionic conductivity of $\text{La}_{1-x}\text{Ni}_{0.5}\text{Ti}_{0.5}\text{O}_{3-\delta}$ is low and has extremely high activation energy, 430 kJ/mol ($x=0.05$) and 222 kJ/mol ($x=0.10$). The atomistic computer simulations showed energetic favorability of defect association, particularly the formation of ternary clusters involving lanthanum and oxygen vacancies and Ni^{3+} . This type of behavior seems responsible for the low ionic and electronic transport.

Acknowledgements

This work was partially supported by the FCT, Portugal (projects POCI/CTM/59197/2004, SFRH/BPD/24639/2005 and SFRH/BPD/15003/2004).

References

- Batiot-Dupeyrat, C., Vanderrama, G., Meneses, A., Martinez, F., Barrault, J. and Tatibouet, J. M., Pulse study of CO_2 reforming of methane over LaNiO_3 . *Appl. Catal. A*, 2003, **248**, 143–151.

2. York, A. P. E., Xiao, T. and Green, M. L. H., Brief overview of the partial oxidation of methane to synthesis gas. *Topics Catal.*, 2003, **22**, 345–358.
3. Kharton, V. V., Yaremchenko, A. A. and Naumovich, E. N., Research on the electrochemistry of oxygen ion conductors in the former Soviet Union II. Perovskite-related oxides. *J. Solid State Electrochem.*, 1999, **3**, 303–326.
4. Rodríguez, E., Álvarez, I., López, M. L., Veiga, M. L. and Pico, C., Structural, electronic and magnetic characterization of the perovskite $\text{LaNi}_{1-x}\text{Ti}_x\text{O}_3$ ($0 \leq x \leq 1/2$). *J. Solid State Chem.*, 1999, **148**, 479–486.
5. Kharton, V. V., Kovalevsky, A. V., Tsipis, E. V., Viskup, A. P., Naumovich, E. N., Jurado, J. R. *et al.*, Mixed conductivity and stability of A-site-deficient $\text{Sr}(\text{Fe,Ti})\text{O}_{3-\delta}$ perovskites. *J. Solid State Electrochem.*, 2002, **7**, 30–36.
6. Hatchwell, C., Bonanos, N. and Mogensen, M., The role of dopant concentration A-site deficiency and processing on the electrical properties of strontium- and titanium-doped lanthanum scandate. *Solid State Ionics*, 2004, **167**, 349–354.
7. Nguyen, T. L., Dokiya, M., Wang, S., Tagawa, H. and Hashimoto, T., The effect of oxygen vacancy on the oxide ion mobility in LaAlO_3 -based oxides. *Solid State Ionics*, 2000, **130**, 229–241.
8. Larson, A. C. and Von Dreele, R. B., General Structure Analysis System (GSAS), Los Alamos National Laboratory Report LAUR 86-748, 2004.
9. Yaremchenko, A. A., Kharton, V. V., Naumovich, E. N., Shestakov, D. I., Chukharev, V. F., Kovalevsky, A. V. *et al.*, Mixed conductivity, stability and thermomechanical properties of Ni-doped $\text{La}(\text{Ga,Mg})\text{O}_{3-\delta}$. *Solid State Ionics*, 2006, **177**, 549–558.
10. Kovalevsky, A. V., Kharton, V. V. and Naumovich, E. N., Oxygen ion conductivity of hexagonal $\text{La}_2\text{W}_{125}\text{O}_{6.75}$. *Mater. Lett.*, 1999, **38**, 300–304.
11. Gale, J. D. and Rohl, A. L., The general utility lattice program (GULP). *Mol. Simul.*, 2003, **29**, 291–341.
12. Naumovich, E. N., Patrakeev, M. V., Kharton, V. V., Islam, M. S., Yaremchenko, A. A., Frade, J. R. *et al.*, Defect interactions in $\text{La}_{0.3}\text{Sr}_{0.7}\text{Fe}(M')\text{O}_{3-\delta}$ ($M' = \text{Al, Ga}$) perovskites: atomistic simulation and analysis of $p(\text{O}_2)$ - T - δ diagrams. *Solid State Ionics*, 2006, **177**, 457–470.
13. Yaremchenko, A. A., Kharton, V. V., Viskup, A. P., Naumovich, E. N., Lapchuk, N. M. and Tikhonovich, V. N., Oxygen ionic and electronic transport in $\text{LaGa}_{1-x}\text{Ni}_x\text{O}_{3-\delta}$ perovskites. *J. Solid State Chem.*, 1999, **142**, 325–335.
14. Kharton, V. V., Yaremchenko, A. A., Shaula, A. L., Patrakeev, M. V., Naumovich, E. N., Logvinovich, D. I. *et al.*, Transport properties and stability of Ni-containing mixed conductors with perovskite- and K_2NiF_4 -type structure. *J. Solid State Chem.*, 2004, **177**, 26–37.
15. Yu, T.-H. and Tuller, H. L., Electrical conduction and disorder in the pyrochlore system $(\text{Gd}_{1-x}\text{Ca}_x)_2\text{Sn}_2\text{O}_7$. *J. Electroceram.*, 1998, **2**, 49–55.
16. Kramer, S., Spears, M. and Tuller, H. L., Conduction of titanate pyrochlores: role of dopants. *Solid State Ionics*, 1994, **72**, 59–66.